Chapter 2
State-of-the-Art of battery State-of-Charge determination

Improvements over time in the use of battery technology and SoC indication will be presented in this chapter. The goal of all the presented SoC determination methods is to arrive at an SoC indication system capable of providing an accurate SoC indication under all realistic user conditions, including those of spread in both battery and user behaviour, a large temperature and current range and aging of the battery. This chapter is organized as follows. Section 2.2 briefly describes the general operational mechanism of batteries and the characteristics of the best-known batteries with their applications. The history of SoC indication is presented in section 2.3. A general State-of-Charge system and possible State-of-Charge indication methods are discussed in sections 2.4 and 2.5, respectively. Section 2.6 focuses on commercially available State-of-Charge systems. Finally, section 2.7 presents concluding remarks.

2.1 Introduction

Humanity has depended on electricity ever since it was first discovered. Without this phenomenon many technological advancements would not have been made. When the need for mobility increased, people switched to portable energy storage devices – first of all wheeled applications, then portable ones and finally wearable use. Several types of rechargeable battery systems are available on the market, such as lead–acid (LA), nickel–cadmium (NiCd), nickel–metal hydride (NiMH), lithium-ion (Li-ion) and lithium-ion polymer (Li-ion POL) batteries. The most important of them will be discussed in this chapter. For almost as long as rechargeable batteries have existed, systems that are capable of indicating the SoC have been around. Several methods for determining the SoC of a battery are known in the art, such as *direct measurements, book-keeping* and *adaptive systems* [1]. An accurate SoC determination method and an understandable and reliable SoC user display will improve a battery's performance and reliability and will ultimately lengthen its lifetime.

2.2 Battery technology and applications

As awkward and unreliable as the early batteries may have been, our descendants may one day look at today's technology in very much the same way as we now view our predecessors' clumsy experiments of 100 years ago [2]. This section focuses on developments in battery technology and characteristics.

In 1800 Volta discovered that a continuous flow of electrical force was generated when certain fluids were used as ionic conductors to promote an

V. Pop et al., *Battery Management Systems. Accurate State-of-Charge Indication for Battery-Powered Applications.*
doi: 10.1007/978-1-4020-6945-1_2, © Springer Science + Business Media B.V. 2008

electrochemical reaction between two metals or electrodes [2]. This led to the invention of the first voltaic cell, better known as a battery.

In 1859 the French physicist Gaston Planté invented the first rechargeable battery. This secondary battery was based on *lead–acid (LA) chemistry*, a system that is still used today. In 1899 the Swedish Waldmar Jungner invented the *nickel–cadmium (NiCd) battery*, based on nickel for the positive and cadmium for the negative electrode. Two years later, Edison came up with an alternative design by replacing cadmium with iron. Due to high material costs relative to dry cells or LA storage batteries, the practical applications of nickel–cadmium and nickel–iron batteries were limited. In 1932 Schlecht and Ackermann invented the sintered pole plate with which great improvements were achieved. These advancements were reflected in higher load currents and improved longevity. The sealed nickel–cadmium battery, as we know it today, only became available in 1947, when Neumann succeeded in completely sealing the cell [2].

Soon after the discovery, in the late 1960s, that intermetallic compounds, such as $SmCo_5$ and $LaNi_5$, were able to absorb and also desorb large amounts of hydrogen [3], it was realized that electrodes made of these materials could serve as a new electrochemical storage medium [4], [5]. In the following years the hydride-forming electrode proved to be a serious alternative to the cadmium electrode, which was widely employed in rechargeable nickel–cadmium batteries. In particular, the higher energy storage capacity, good rate capability and non-toxic properties of the chemical elements of which these hydride-forming materials were composed were great advantages in relation to the cadmium electrode [6]. The *nickel–metal hydride (NiMH) battery* became commercially available in the 1990s [7].

The first non-rechargeable *lithium batteries* appeared in the early 1970s. Attempts to develop rechargeable lithium batteries followed in the 1980s but failed due to safety problems. Because of the inherent instability of lithium metal, especially during charging, research shifted to intercalate lithium ions in host materials in Li-ion batteries. Although lower in energy density than lithium metal, lithium ion is safe, provided certain precautions are taken when charging and discharging, implemented by means of a proper charging algorithm and a safety IC in series with the battery as discussed in the previous chapter. In 1991, the Sony Corporation commercialised the first *lithium-ion battery (Li-ion)* [1].

Table 2.1 summarises the history of the battery developments described above. The general operational mechanism of a battery and characteristics of the most important rechargeable batteries available on the market today, *e.g. nickel–cadmium, nickel–metal hydride* and *lithium-ion batteries*, will be given in the remainder of this section.

Table 2.1. History of battery development [2].

Year	Researcher (Country)	Method
1800	Volta	Invention of the battery
1859	Plante (France)	Invention of the lead-acid battery
1899	Jungner (Sweden)	Invention of the nickel-cadmium battery
1901	Edison (USA)	Invention of the nickel-iron battery
1932	Schlecht & Ackermann (Germany)	Invention of the sintered pole plate
1947	Neumann (France)	Successful sealing of the nickel-cadmium battery
1990	Sanyo (Japan)	First commercial introduction of the NiMH battery
1991	Sony (Japan)	First commercial introduction of the Li-ion battery

2.2.1 General operational mechanism of batteries

In its simplest definition, a battery is a device capable of converting chemical energy into electrical energy and *vice versa*. The chemical energy is stored in the electroactive species of the two electrodes inside the battery. The conversions occur through electrochemical reduction-oxidation (redox) or charge-transfer reactions [1]. These reactions involve the exchange of electrons between electroactive species in the two electrodes through an electrical circuit external to the battery. The reactions take place at the electrode/electrolyte interfaces. When current flows through the battery, an oxidation reaction will take place at the anode and a reduction reaction at the cathode. The oxidation reaction yields electrons to the external circuit, while a reduction reaction takes up these electrons from the external circuit. The electrolyte serves as an intermediate between the electrodes. It offers a medium for the transfer of ions. Hence, current flow is supported by electrons inside the electrodes and by ions inside the electrolyte. Externally, the current flows through the charger or load [1]. The basic electrochemical unit of a battery is called a *cell*, but the word *battery* is commonly used for one cell or for two or more cells connected in series/parallel.

During a battery's lifetime, its performance or 'health' tends to deteriorate gradually due to irreversible physical and chemical changes that take place with usage and with age until the battery is finally no longer usable. The State-of-Health (SoH) is an indication of the point that has been reached in a battery's life cycle and a measure of its condition relative to that of a fresh battery. Aging of the battery is a complex process that involves many battery parameters (*e.g.* impedance, capacity), the most important of which is capacity. To illustrate the phenomena, Fig. 2.1 shows the discharge capacity (Q_d) of a Li-ion battery represented as a function of the cycle number (C_n). The degradation curve has a clearly visible transfer point at which the rate of the battery's degradation increases.

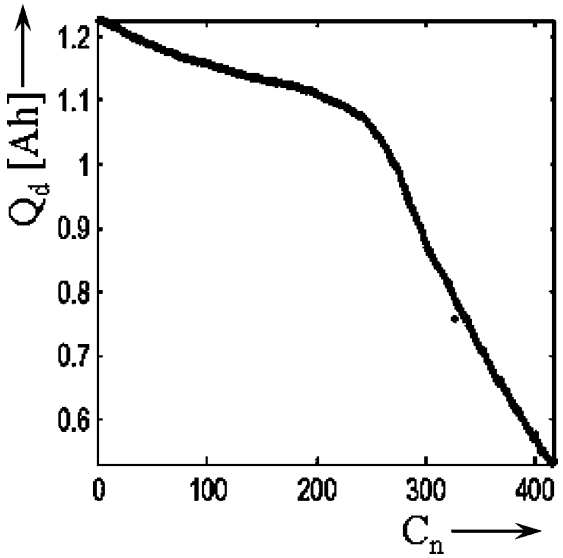

Fig. 2.1. Decrease of the discharge capacity Q_d [mAh] as a function of the operational conditions. The horizontal axis shows the cycle number C_n.

The exact position of the transfer point varies, depending on the type of battery and operational conditions. Aging of Li-ion batteries is not an absolutely new topic in modern electrochemistry. A number of models describing the aging effects in Li-ion batteries have recently been introduced. Models describing the dynamics of lithium consumption in Li-ion batteries are discussed by Broussely and Spotnitz in [8], [9]. Both Broussely and Spotnitz deal with the aging of the batteries under 'on float' condition, with the battery being kept under constant voltage of fixed polarity. A striking feature of all plots in the aforementioned articles is that they are smooth and do not have any transfer points.

A first conclusion is that it will be difficult to take into account every nuance of a battery's charge and discharge qualities and aging characteristics in an SoC indication system.

2.2.2 Battery types and characteristics

NiCd batteries. Batteries based on a positive nickel electrode of a $Ni(OH)_2$/NiOOH compound and a negative cadmium electrode of Cd and $Cd(OH)_2$ are called NiCd batteries. The electrolyte is an aqueous KOH solution. A great advantage of NiCd batteries is their fast charge and discharge performance: it is possible to charge a battery in 10 minutes and large currents can be supplied during discharge. NiCd batteries have an average operating voltage of 1.2 V and can be used in many devices. NiCd batteries are used especially in tools demanding a lot of power. Other applications include cordless and mobile phones, shavers, camcorders, portable audio products and laptop computers. Disadvantages of NiCd batteries are their relatively low energy density and their so-called memory effect. This memory effect causes the battery to deliver only the capacity used during the preceding repeated charge/discharge cycles. Because of this effect the entire capacity of NiCd batteries should preferably be used for each discharge cycle to avoid a decrease in

the maximum capacity [1]. Another disadvantage is the presence of cadmium, which is an environmental hazard. This will lead to a complete ban on NiCd batteries in the future.

NiMH batteries. The main difference between NiCd and NiMH batteries is the fact that in NiMH batteries a metal hydride alloy is used for the negative electrode instead of cadmium. In this way a higher energy density is obtained and the memory effect and environmental impact are reduced. NiMH batteries can moreover replace NiCd batteries because they have the same 1.2 V average operating voltage per cell. Applications include cordless and mobile phones, shavers, camcorders, portable audio products, laptop computers and Hybrid Electrical Vehicles (HEVs). A disadvantage of NiMH batteries is their relatively high self-discharge rate and relatively poor robustness with respect to overcharging, which is made worse by the fact that it is more difficult to detect the battery-full condition during charging [1].

Li-ion batteries. A schematic representation of a typical Li-ion cell is shown in Fig. 2.2 [10]. The cell consists of five regions (from left to right in Fig. 2.2): a negative-electrode current collector made of copper, a porous composite negative insertion electrode, a porous separator, a porous composite positive insertion electrode and a positive-electrode current collector made of aluminium. The composite electrodes are made of active material particles held together by a binder and a suitable filler material such as carbon black. When discharge is about to begin the negative electrode is fully lithiated and the positive electrode is ready to accept lithium ions. During discharge, the lithium ions deintercalate from the negative electrode particles and enter the solution phase, while in the positive electrode region lithium ions in the solution phase intercalate into the $LiCoO_2$ particles. This results in a concentration gradient, which drives lithium ions from the negative electrode to the positive electrode. The cell voltage decreases during discharge, as the equilibrium potentials and overpotentials of the two electrodes are strong functions of the concentrations of lithium on the surface of the electrode particles. The cell is considered to have reached the end of discharge when its voltage drops to 3.0 V [10].

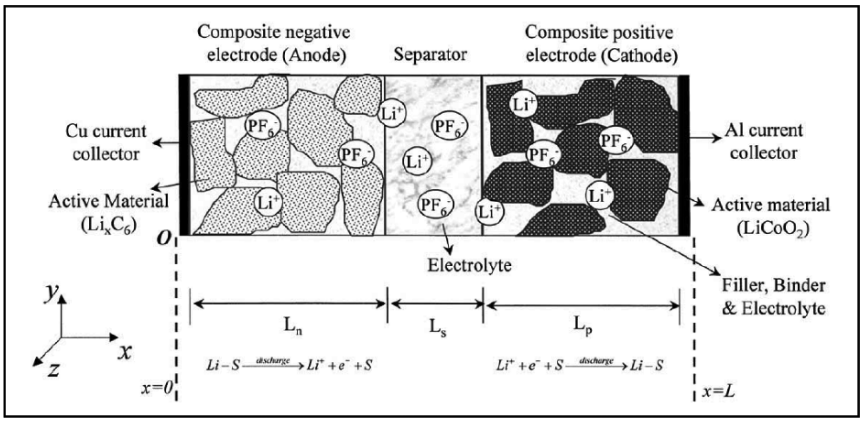

Fig. 2.2. A schematic representation of a typical Li-ion cell [10].

The positive electrode is made of lithium metal oxides (*e.g.* $LiCoO_2$, $LiNiO_2$ or $LiMn_2O_4$) for storing the lithium ions. The negative carbon electrode is made of graphite or petroleum coke. The electrolyte is usually a salt dissolved in an organic solvent, but batteries with other solvents such as propylene carbonate also exist. An example of an employed salt is $LiPF_6$. The operating voltage of the Li-ion batteries is critical and over(dis)charging results in fast aging and may cause fire or even exploding batteries. As discussed in chapter 1, an essential electronic protection circuit is consequently required to prevent over(dis)charging. Applications include mobile phones, shavers, camcorders, portable audio products and laptop computers.

2.2.3 Summary

Several types of rechargeable battery systems have been discussed in this section. The main characteristics of the discussed battery types are summarised in Table 2.2 [1].

Table 2.2. Overview of the main characteristics of the most important rechargeable battery systems.

Battery system	NiCd	NiMH	Li-ion
Average operating voltage (V)	1.2	1.2	3.6
Energy density (Wh/l)	90 – 150	160 – 310	200 – 280
Specific energy (Wh/Kg)	30 – 60	50 – 90	90 – 115
Self-discharge rate (%/month) at 20°C	10 – 20	20 – 30	1 – 10
Cycle life	300 – 700	300 – 600	500 – 1000
Temperature range (°C)	–20 – 50	–20 – 50	–20 – 50

2.3 History of State-of-Charge indication

In this section, previous and current SoC technologies will be presented. For almost as long as rechargeable batteries have existed, systems capable of indicating the amount of charge available inside a battery have been around. In 1938 Heyer introduced a single-meter device on which the value of a storage battery capacity is indicated [11]. The battery capacity is indicated on the basis of the measured battery voltage and a measured voltage drop across a sense resistor. When the battery is fully charged the device indicates 100% capacity (see Fig. 2.3). A simple test is done to determine when the battery should be replaced. In this test the voltage drop across a sense resistor during discharge from 100% capacity is measured. It is assumed that the voltage drop will be small in a fresh battery and high in an aged battery, implying that the battery should be replaced. Replacement is required when the battery capacity falls below 70% in the discharge test (see Fig. 2.3).

In 1963 Curtis Instruments pioneered gauges for monitoring the SoC, the ‘fuel’ level, of vehicle traction batteries. One of the methods used by Curtis involves predicting a battery’s remaining capacity by measuring the amount of time elapsed since the loaded voltage dropped below a certain value. For example, when a battery is discharged from 24.25 V for a period of 3 minutes, the remaining capacity falls from 100% to 90%, *etc.* [12]. A compensation method for different discharge rates is also presented.

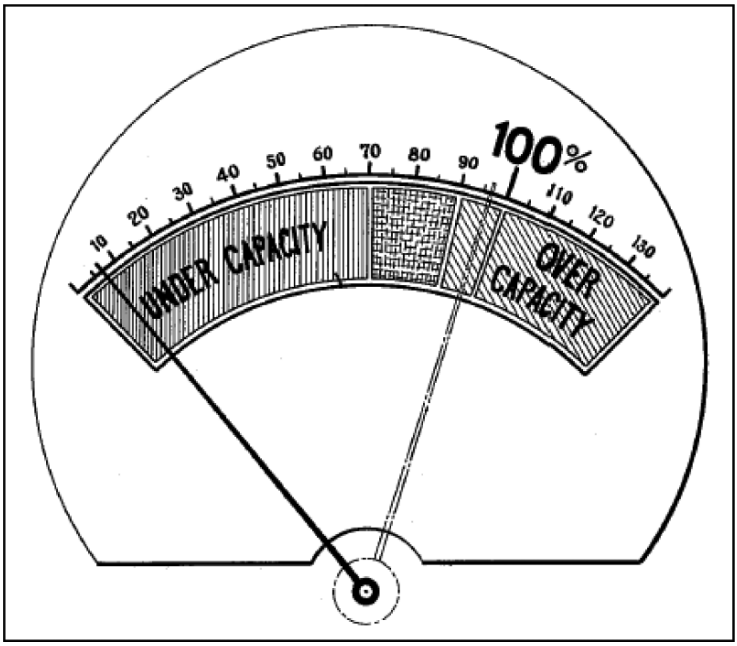

Fig. 2.3. Battery capacity indicator developed by Heyer (1938) [11].

Several monitors based on the average voltage were available in those days, such as Sears battery monitor, a range indicator (by Motovator) and the aforementioned Curtis fuel gauge. Of these, the Curtis fuel gauge was found to be the most sophisticated and accurate [13]. Curtis SoC gauges were even used on the Moon (see Fig. 2.4) [14].

Fig. 2.4. Astronauts exploring the Moon in Lunar Roving Vehicles in 1971–1972 relied on early Curtis gauges [14].

In one of the Curtis patents filed by Finger *et al.* in 1975 the current flowing from the battery is sent to an integrator module, which registers the current depletion [15]. During charging, the current is integrated in the integrator module providing a continuous display of the SoC and information needed to regulate the charge rate.

An account of the attempts made to develop an SoC indicator for a nickel–cadmium battery was given by Lerner in 1970 [16]. He concluded that the only reliable way of estimating the SoC is to use a current-sharing method. In this method, the current output of a battery having a known SoC is compared with that of a battery having an unknown SoC. The SoC of the unknown battery can be deduced from the outcome of this comparison.

In 1974 York *et al.* introduced an SoC indicator in which the value of the measured battery voltage is indicated with respect to two voltage levels stored in the system [17]. In a first state it is indicated that the battery voltage is greater than a first voltage level and in a second state it is indicated that the battery voltage is less than the first voltage level but greater than a second voltage level. Finally, a third state indicates that the battery voltage is less than the second voltage level and disables the load connected to the battery. The magnitude and duration of the voltage reduction are monitored by a threshold circuit, which produces an output whenever the terminal voltage falls below the lower threshold value. As a response to the voltage reduction, a number of pulses are generated. An electronic counter is used for counting the pulses and accumulating the counts. An integral proportional to the total time that the terminal voltage is below the lower threshold voltage is generated. The output of the integration provides an indication of the SoC. A principal advantage of this method is that SoC can be indicated despite sudden disconnection and reconnection of a battery.

The main concept of determining a battery's SoC on the basis of a comparison between the measured battery voltage and predetermined threshold values that correspond to different SoC values is also presented in [18]–[20]. In [18] the average current consumption of a portable device is determined by using a capacitor for energy storage. The capacitor is charged and discharged between two voltage thresholds in a certain measured time. The number of charging processes occurring in the measured time are counted and used to calculate the average current consumption. The maximum error obtained for the average current calculation using the above method was smaller than 5% [18]. In [19] it is shown that the approximation of the accumulated operating time of a rechargeable battery is a function of the internal resistance of the rechargeable battery. The SoC is measured relative to the rechargeable battery's maximum capacity. The applications presented in [18], [19] are described in the field of mobile telephony. In [20] voltage levels are measured during battery charge and discharge and compared with predetermined values, which are modified as a function of temperature. The stored battery charge or discharge curves are divided into curve portions defined by voltage levels and rates of changes of the voltage levels. Each curve portion defines a particular SoC of the battery. Measured voltage levels and rates of changes are then associated with the predetermined charge or discharge curve portion and the defined SoC.

In 1974 Brandwein *et al.* developed a device for monitoring nickel–cadmium batteries [21]. In addition to voltage measurements, the current that flows into and out of the battery and the battery temperature are measured and used in order to provide SoC indication. The battery voltage is stored as an analog voltage signal at

different temperatures. [22] presents an equivalent circuit diagram of the battery that uses current, voltage and temperature measurements as inputs. The measured values are compared with the corresponding values obtained in calculations using the equivalent circuit diagram. The parameters in the equivalent circuit diagram and the state variables are varied so that the measured values are matched and the SoC can be inferred from the adjusted parameters.

In 1975 Christianson *et al.* developed a method in which a battery's SoC is indicated on the basis of the open-circuit voltage (OCV) calculation [23]. The OCV is directly proportional to the battery SoC and can be calculated using the following equation:

$$OCV = V_{bat} + IR \tag{2.1}$$

where V_{bat} is the battery terminal voltage, I the actual battery current – regarded as a positive value during discharge and a negative value during charge – and R is the internal resistance. Note that OCV = V_{bat} when $I = 0$, but after current interruption this takes a while due to several relaxation processes occurring inside a battery. In addition to the OCV, the method presented by Eby *et al.* in 1978 also uses the voltage under load to determine the SoC of an LA storage battery during a discharge cycle [24]. The battery's initial OCV is stored in a settable memory. It has been demonstrated that in the case of LA batteries the OCV has a linear correlation to the charge level of the battery under a defined set of circumstances. The discharge rate can be determined at any moment in time as a comparison function between voltage under load and the corresponding OCV.

The first impedance measurements of batteries appear to have been made by Willihnganz in 1941 [25]. They involved excitation of the electrochemical cell by an ac voltage of small amplitude of about 5 mV and evaluation of the resistive and reactive components or other related parameters such as the modulus of impedance and phase angle. As such measurements encompass a wide range of ac signal frequencies, various characteristic parameters of the electrochemical cell and the kinetics of the associated reactions can be evaluated [25]. As an alternative, Dowgiallo *et al.* (1975) and Zaugg (1982) developed methods for determining a battery's SoC on the basis of impedance measurements [26], [27]. The phase angle between the ac voltage across the battery terminals and the ac current through the battery (measured as a voltage through a sense resistor) is continuously monitored. The method presented in [26] relates to nickel–cadmium batteries and can be used in equipment such as transmitters, receivers, tape recorders, movie cameras, aircraft, electric vehicles, small calculators and computers. In the system developed by Muramatsu in 1985 the relationships between the battery impedance at different frequencies (defined as impedance spectroscopy), remaining capacity and SoH are used to detect a battery's SoC and SoH [28]. Predetermined values based on this relationship are stored in look-up tables and used to determine the battery's SoC and SoH. Look-up tables are tables in which fixed values of measured parameters, such as voltage, current, impedance and temperature, can be stored and used in order to indicate the SoC.

In 1984 Peled developed a method for determining the SoC of lithium-ion batteries [29]. The presented method is based on predetermined voltage and temperature measurements that are used as input parameters for look-up tables. After a current step and a short resting period, a battery's OCV and temperature are measured. The measured value is compared with a corresponding predetermined

value stored in a look-up table. The outcome of this comparison is used to indicate the SoC. In the system developed by Kopmann (1987) the terminal voltage, the current and time are measured during each battery charging and discharging cycle [30]. These values are also used as inputs for look-up tables. The characteristic of the terminal voltage curve during charging and discharging is used to minimise the differences between the measured values and the battery's actual SoC. [31] presents a method for determining the SoC of NiMH batteries in notebook applications. The method uses the battery's temperature, voltage and discharge/charge rate measurements to determine the SoC, using look-up tables. A possible hardware and software implementation is also presented. These techniques can be employed for any other battery technology by modifying the look-up tables.

In 1981 Finger of Curtis Instruments patented a method according to which the SoC of Lead-Acid (LA) batteries is determined during a quiescent interval with no current flowing through the battery [32]. The battery terminal voltage is measured after a current step and the combination of these two measurements (battery voltage and time) is used for battery OCV recovery characteristics determination. This predictable time function of voltage recovery is substantially independent of the actual voltage level of the terminal voltage.

[33] presents an SoC indicator for a lithium-ion battery based on a cell OCV. The SoC is calculated on the basis of a stored SoC–OCV relationship. The SoC–OCV relationship is obtained by defining the battery charge amount when the OCV of the cell is 3.9 V as SoC = 100% and defining the battery charge amount when the OCV of the cell is 3.5 V as SoC = 0%. By defining SoC = 100% and SoC = 0% the SoC can be correctly calculated and displayed even when a battery ages.

The methods presented in [34]–[38] use Coulomb counting, *i.e*. battery current measurement and integration, as a basis. The method developed by Aylor (1992) holds for LA batteries [34]. The described technique is a combination of the previously described OCV method and coulometric measurements (Coulomb counting). The paper states that it is possible to compensate for the weakness of both techniques and provide an accurate SoC indication by combining these two measurements. Coulometric measurements are used in short time operations, in which the accumulation of error is negligible. The error that is accumulated in coulometric measurement techniques can be corrected by taking an OCV reading every time the battery has rested sufficiently. A method for predicting the OCV before the battery voltage has fully stabilised has been developed in order to reduce the required rest period of the OCV measurements. It should be noted that this method is limited to LA-type batteries because of the unique linear relation between the OCV and the specific gravity that exists in LA batteries. In [39] it is indicated that the method presented in [34] could provide 99% accuracy (1% error) for charge detection, but at a high cost of realization. The application described in [37] relates to a battery pack using NiMH batteries or any other battery technology such as LA, lithium polymer, *etc.*, operating in a hybrid–electric power train for a vehicle. Besides Coulomb counting, the systems presented by Kikuoka [35] and Seyfang [36] also compensate for temperature, charging efficiency of the battery, self-discharge and aging. In [36] a battery's capacity is monitored and compared with the initial capacity to obtain an indication of the battery's SoH. When the battery is fully discharged or fully charged a particular set of parameters, such as the conversion efficiency of each battery, are 'learned' and updated to take into account the battery's aging. Besides Coulomb counting and voltage, current and

temperature measurements, [38] presents a mathematical model that is implemented on a computer that simulates a battery's behaviour.

The methods presented in [40]–[42] also use adaptive methods for determining a battery's SoC. In 1997 Gerard *et al.* developed a method in which a battery's 'state variables' are replaced with neural weights with the aim of providing portable equipment users with an accurate estimation of the remaining working time, *e.g.* how much time is left until the battery voltage reaches the end-of-discharge voltage defined in a portable device [40]. Two artificial neural networks are used to model the system's implementation, more precisely, to adapt the prediction of the current discharge curve to the general behaviour of the employed battery pack. A mean error of about 3% has been found using this implementation method. In 1999 Salkind *et al.* developed a method for SoC and SoH prediction based on fuzzy logic modelling for two battery systems – lithium–sulphur dioxide (Li-SO_2) and NiMH [41]. The method involves the use of fuzzy logic mathematics to analyse data obtained by impedance spectroscopy and/or Coulomb counting techniques. The maximum error between the measured SoC and the model-predicted SoC obtained using the above method for a limited data set in the case of lithium–sulphur dioxide cells was +/– 5%. In 2000 Garche *et al.* developed a method in which the Kalman filters (KF) are used to implement an adaptive method in connection with parameter estimation to determine SoC [42]. The basis of the filter is a numeric battery model description. The battery voltage is estimated on the basis of the current and temperature measurements and the results are compared with the measured battery voltage value. Adaptivity of the model is based on a comparison of the estimated values with observed battery behaviour. A more detailed description of these adaptive methods will be given in section 2.5.

In 2000 Bergveld *et al.* developed a method for estimating the SoC of a rechargeable lithium-ion battery [1], [43]. The basis of the algorithm is current measurement during the charge or discharge state and voltage measurement during the equilibrium state (state in which no current is flowing into or out of the battery and all the conditions inside the battery are fully stabilised). In the charge and discharge states the determination of the SoC relies on calculating the charge withdrawn from or supplied to the battery by means of current integration and subtracting this charge from or adding it to the previously calculated SoC. So in these states Coulomb counting is applied and the battery is viewed as a simple linear capacitor.

In addition to simple Coulomb counting the effect of the overpotential is also considered in the discharge state. Due to this overpotential, the battery voltage during discharging is lower than the Electro-Motive Force (EMF equals the sum of the equilibrium potentials of a battery's electrodes), which in equilibrium equals the OCV presented above. The value of the overpotential depends on the discharge current, the SoC, age and temperature. Especially at low temperatures and low SoC values the remaining charge cannot be withdrawn from the battery due to a high overpotential caused mainly by diffusion limitation of the electrochemical reactions, because otherwise the battery voltage will drop below the end-of discharge voltage defined in the portable device. This leads to an apparent capacity loss, which at low temperatures of *e.g.* 0°C may amount to more than 5%. So a distinction should be made between the charge that is available in the battery and the charge that can be withdrawn from the battery under certain conditions. As overpotentials are temperature dependent, temperature measurements must also be carried out in the discharge state [1].

In the equilibrium state, a battery's SoC is determined by means of voltage measurements. Because only a negligibly small current flows in this state, the measured voltage approaches the battery's EMF. The algorithm uses a stored EMF versus-SoC curve to translate a measured voltage value into an SoC value expressed in % of the maximum capacity. The EMF-versus-SoC curve remains the same even when the battery ages and the temperature dependence of this curve is relatively low [1], [44]. The EMF method can also be used to calibrate the SoC system because the same SoC has been found for a certain measured EMF, irrespective of the battery's age and temperature. This calibration is important, because in the charge and discharge states the calculated SoC will eventually drift away from the real value due to *e.g.* measurement inaccuracy in the current and the integration in time of this inaccuracy [1]. A complete description of this algorithm, which is also the starting point of this book, will be given in the next chapter.

Table 2.3 summarises the most important points of the history of SoC development outlined above.

Table 2.3. History of SoC development.

Year	Researcher/ Company	Method
1938	Heyer	Voltage measurements
1963	Curtis	Voltage measurements and threshold in voltage levels
1970	Lerner	Comparison between two batteries (one with a known SoC)
1974	Brandwein	Voltage, temperature and current measurements
1975	Christianson	OCV
1975	Dowgiallo	Impedance measurements
1975	Finger	Coulomb counting
1978	Eby	OCV and voltage under load
1980	Kikuoka	Book-keeping
1981	Finger	Voltage relaxation
1984	Peled	Look-up tables based on OCV and T measurements
1985	Muramatsu	Impedance spectroscopy
1986	Kopmann	Look-up tables based on V, I and T measurements
1988	Seyfang	Book-keeping and adaptive system
1992	Aylor	OCV, OCV prediction and coulometric measurements
1997	Gerard	Voltage and Current Measurements, Artificial Neural Networks
1999	Salkind	Coulomb counting, impedance spectroscopy, fuzzy logic
2000	Garche	Voltage and Current Measurements, Kalman filters
2000	Bergveld	Book-keeping, overpotential, EMF, maximum capacity learning algorithm

As will be shown later in this chapter, the actual State-of-Charge indication integrated circuits (ICs) are based on the methods indicated in this table. More detailed information on the applied methods will be given in section 2.5.

2.4 A general State-of-Charge system

In science, the standard unit used to express battery capacity is Coulomb (named after the French physicist C. A. Coulomb, 1736–1806), which describes the time a battery can produce a given current. The Coulomb is the unit of electric charge corresponding to one ampere-second (As). In practice, however, cell or battery capacity is more commonly expressed in ampere-hours (Ah) or milliampere-hours (mAh). Of great importance for users is to know a battery's SoC. In [37] SoC is defined as the percentage of the full capacity of a battery that is still available for further discharge. In [25] it is the ratio of a cell's available capacity and its maximum attainable capacity. For a proper understanding of what the term 'SoC' really implies a clear definition is needed: SoC is the percentage of maximum possible charge that is present inside a rechargeable battery. The SoC measurement method and the computational model based on the correct SoC definition must be simple, convenient, practical and reliable.

Fig. 2.5 shows an example of a practical SoC system. The battery may include a plurality of battery cells connected in series and/or parallel, each of the battery cells having at least two terminals. The SoC system may include an analogue-to-digital converter (ADC) for converting a voltage drop between at least two sense resistor connection pins as a measure of the current *(I)* into a digital signal and also for converting the measured analogue values of the battery voltage *(V)* and temperature *(T)* into digital signals.

A microprocessor/microcontroller (in which the SoC algorithm is stored) determines a battery system's SoC on the basis of the measured signals. Two types of memory are needed. Basic battery data, such as the amount of self-discharge as a function of *T* and the discharging efficiency as a function of *I* and *T*, are read from the read-only memory (ROM). When the SoC algorithm is based on EMF measurements, the EMF–SoC relationship can be stored in ROM together with other battery-specific data. The random access memory (RAM) is used to store the history of use, such as the number of charge/discharge cycles, which can be used to update the maximum battery capacity. Each part of this system (software algorithm or hardware device) will influence the ultimate accuracy of the SoC indication (*e.g.* inaccuracy in the *V*, *T* and *I* measurements will result in inaccuracy in the final SoC). Also important is the calibration of the SoC, because if the SoC algorithm is based on, say, current measurement and integration, the error caused by the current measurement inaccuracy will accumulate over time.

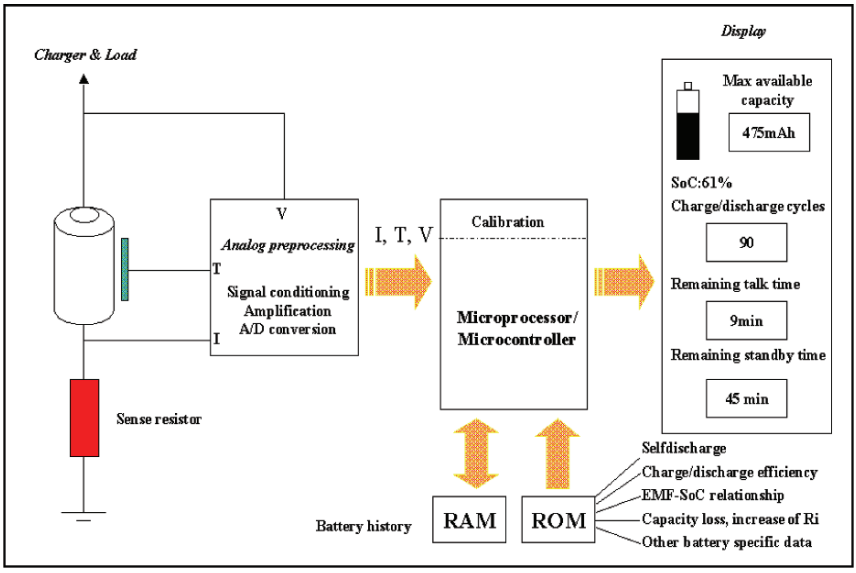

Fig. 2.5. General functional architecture of a State-of-Charge system.

2.5 Possible State-of-Charge indication methods

For an efficient discussion of SoC indication methods, some of the terms commonly used in the battery SoC industry should be defined.

Ampere-hour. A measure of electric charge defined as the integral product of current (in Amperes) and time (in hours).

Cell. The basic electrochemical unit used to generate electrical energy from stored chemical energy or to store electrical energy in the form of chemical energy. A cell consists of two electrodes in a container filled with an electrolyte.

Battery. Two or more cells connected in an appropriate series/parallel arrangement to obtain the operating voltage and capacity required for a certain load. The term is also frequently used for single cells.

Li-ion cells. Cells containing a liquid organic or polymer electrolyte in which the anode and cathode are both made of intercalation compounds [46].

C-rate. A charge or discharge current equal in Amperes to the rated capacity in Ah. Multiples larger or smaller than the C-rate are used to express larger or smaller currents. For example, the C-rate is 1100 mA in the case of an 1100 mAh battery, while the C/2 and 2C-rates are 550 mA and 2.2 A, respectively.

Capacity. A battery's electrical energy content expressed in ampere-hours.

Maximum capacity. Maximum amount of capacity that can be removed from a battery under defined discharge conditions.

Cycle life. The number of cycles that a cell or battery can be charged and discharged under specific conditions before the available capacity in Ah fails to meet specific performance criteria. This will usually be 80% of the rated capacity.

Cut-off voltage. The lowest operating voltage at which a cell is considered depleted. Also often referred to as end-of-discharge voltage or final voltage [34].

Self-discharge. The recoverable loss of a cell's useful capacity on storage due to internal chemical action. This is usually expressed in a percentage of the rated capacity lost per month at a certain temperature because batteries' self-discharge rates are strongly temperature-dependent. The self-discharge mechanism is a local redox process caused by decomposition of the electrolyte [46]. Other important sources for the self-discharge are micro-shorts and shuttle-molecules.

Spread. Difference between characteristics of batteries of the same type.

State-of-Health (SoH). A 'measurement' that reflects a battery's general condition and its ability to deliver the specified performance in comparison with a fresh battery.

State-of-Charge (SoC). The percentage of the maximum possible charge that is present inside a rechargeable battery.

Depth-of-Discharge (DoD). The amount of capacity withdrawn from a battery expressed as a percentage of its maximum capacity.

Depth-of-Charge (DoC). The amount of capacity put into a battery expressed as a percentage of its maximum capacity.

Remaining run-time. The estimated time that a battery can supply current to a portable device under valid discharge conditions before it will stop functioning.

As indicated in section 2.3, there are several methods for determining the SoC of a battery. Some early, very inexpensive fuel gauges simply measured voltage. Battery voltage is a highly inaccurate indication of a battery's capacity because it changes with temperature, discharge rates and aging. Another known method for measuring SoC involves impedance measurements. The measurements obtained are compared with previously generated standard reference curves. Yet another prior-art method used to determine battery SoCs involves estimating the SoC on the basis of a battery's response to current or voltage pulses. These pulse systems yield only a very general impression of a SoC and are used primarily to determine whether a battery is still useable. This first group of methods will be called *direct measurements* below.

Another known method is to measure the current flowing into and out of a battery and to integrate this current over time in order to determine its capacity [1]. When using these current integrators one must correct the estimation of the SoC obtained because several battery-related factors affect the accuracy of the

estimation. These factors include temperature, history, charge and discharge efficiencies and cycle life. The integration of current is referred to in the literature as *Coulomb counting* [1]. When discharging 'efficiency', self-discharge and capacity loss are compensated for, this method can be regarded as a *book-keeping* system [1].

The main problem in designing an accurate SoC indication system is the unpredictability of the behaviour of both batteries and users. For this reason use must be made of an adaptive system based on direct measurement, book-keeping or a combination of the two [1]. In order to clarify all aspects, these methods will be discussed separately below.

2.5.1 Direct measurement

The direct measurement method refers to the measurement of battery variables such as the battery voltage (V), battery impedance (Z) and voltage relaxation time (τ) after application of a current step. Most relations between battery variables and the SoC depend on the temperature (T). This means that the battery temperature should also be measured, besides the voltage or impedance. The basic principle of a SoC indication system based on direct measurement is shown in Fig. 2.6.

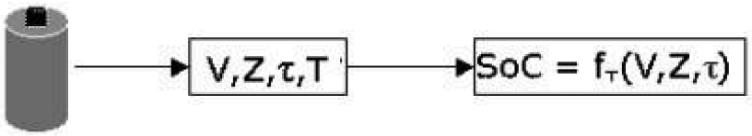

Fig. 2.6 Basic principle of a SoC indication system based on direct measurement.

The main advantage of a system based on direct measurement is that it does not have to be continuously connected to the battery. The measurements can be performed as soon as the battery has been connected [1].

Voltage measurements. Although voltage measurement has been a popular method, especially for mobile phone applications, it does not produce the most accurate results. Determining the remaining capacity of a cell simply by measuring its voltage level may be less expensive and may use less computing power of the host CPU than Coulomb counting, but under real-life conditions voltage measurements alone can be very misleading [47]. While it is true that a given cell voltage level will continually drop during discharge, the voltage level in relation to remaining charge varies greatly with cell temperature and discharge rate. Fig. 2.7 shows an Li-ion battery voltage curve during discharge at different discharge rates.

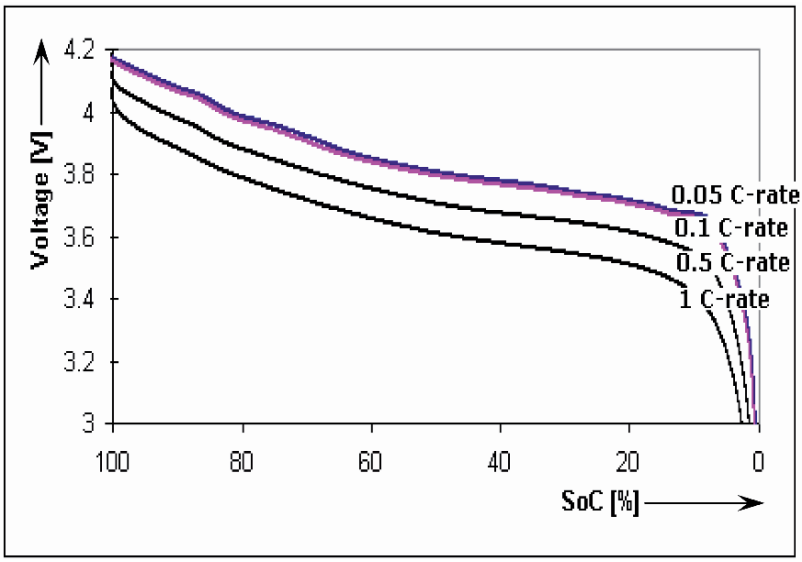

Fig. 2.7. Li-ion battery voltage curves at different discharge rates.

The important point illustrated in Fig. 2.7 is the relationship between the cell voltage and its discharged capacity. It can be seen that the voltage discharge curve depends strongly on the discharge rate. The error in SoC estimation based on voltage measurement can be corrected by the system if the dependence of the battery voltage on the cell temperature and discharge rate is known. However, when those measured curves are included the process becomes more complicated and expensive than a Coulomb counting approach [47].

The EMF method. The term EMF stands for electromotive force. It is a battery's internal driving force for providing energy to a load. In principle, the EMF can be inferred from thermodynamic data and the Nernst equation (or equations derived from it) [1]. Another method with which the EMF can be obtained is called *linear interpolation*. With this method the average battery voltage, calculated at the same SoC, is inferred from the battery voltages during two consecutive discharge and charge cycles using the same currents and at the same temperature. Fig. 2.8 shows the EMF curve obtained at 25°C with the linear interpolation method using Sony's US18500G3 Li-ion battery.

In another known method the EMF is determined on the basis of *voltage relaxation*. The battery voltage will relax to the EMF value after current interruption. This may take a long time, especially when a battery is almost empty, at low temperatures and after a high discharge current rate [44]. In another EMF determination method – *linear extrapolation* – the battery voltages obtained with different currents with the same sign and at the same SoC value are linearly extrapolated to a current of value zero [1].

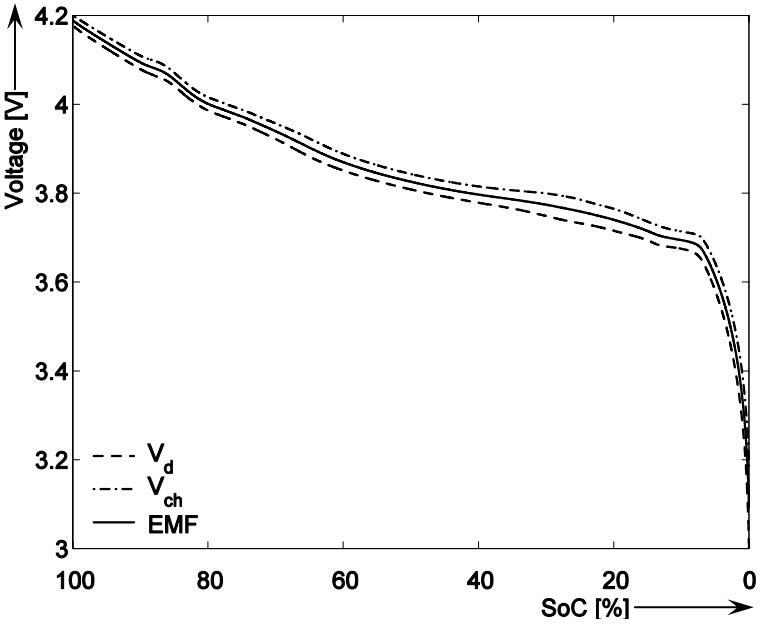

Fig. 2.8. EMF curve obtained with the linear interpolation method.

The EMF of an Li-ion battery has been found to be a good measure of battery SoC. It has been demonstrated that the relationship between the EMF and the SoC does not change during cycling of the battery if the SoC is expressed in relative capacity [1]. The temperature dependence of the EMF is small, except when the battery is almost fully discharged or almost fully charged.

When the SoC algorithm is based on the EMF an accurate method for EMF implementation is required. Three of the EMF implementation methods used in practice will be presented below.

(a) *Look-up table.* A table in which fixed values of the measured parameters can be stored and used in order to indicate SoC. The size and accuracy of the look-up tables in SoC indication systems depend on the number of stored values. One of the main drawbacks of this method is that even in the case of a single type of battery it is difficult to take into account every point of the EMF curve in order to provide an accurate SoC indication system. When many measurement points are included the process becomes more complicated and expensive than other approaches, and will probably not provide any significant advantages.

(b) *Piecewise linear function.* In this method the EMF curve is approximated with piecewise linear functions. A possible example with 10 intervals is shown in Fig. 2.9 for Sony's US18500G3 Li-ion battery. The intervals in voltage and the corresponding SoC are presented in Table 2.4.

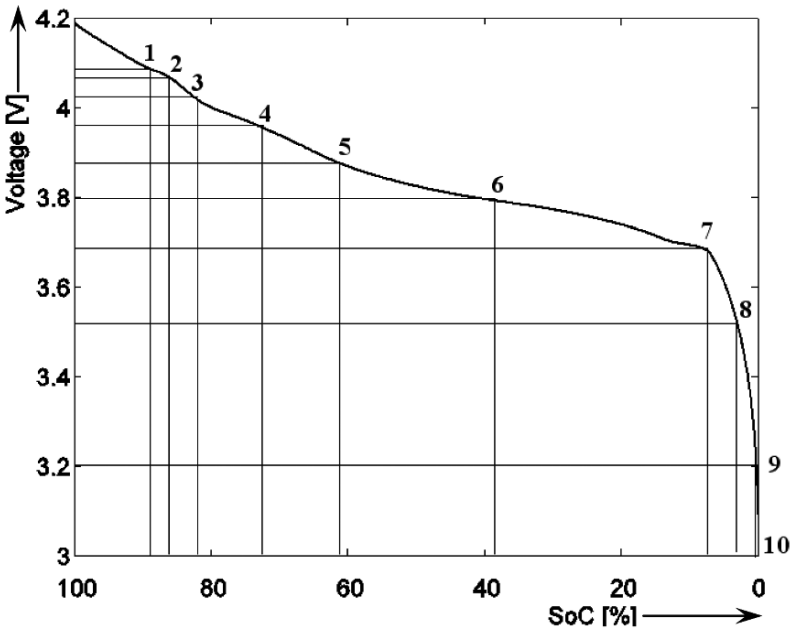

Fig. 2.9. Piecewise EMF curve for the US18500G3 Li-ion battery from Sony.

Table 2.4. Possible EMF curve implementation (see also Fig. 2.9).

Interval number	Interval voltage limits [V]	SoC [%]
1	4.08 – 4.20	90 – 100
2	4.06 – 4.08	84 – 90
3	4.02 – 4.06	81 – 84
4	3.98 – 4.02	72 – 81
5	3.88 – 3.98	61 – 72
6	3.80 – 3.88	39 – 61
7	3.68 – 3.80	8 – 39
8	3.54 – 3.68	4 – 8
9	3.22 – 3.54	0.5 – 4
10	3.00 – 3.22	0.0 – 0.5

With the aid of Eq. (2.2), the SoC for any measured battery equilibrium voltage value, *i.e.* EMF, can be calculated:

$$SoC = SoC_l + \frac{EMF - V_l}{V_h - V_l}(SoC_h - SoC_l) \tag{2.2}$$

where V_l and V_h are fixed and specific values from the EMF curve representing the voltages corresponding to the SoC_l [%] and SoC_h [%] SoC values, *e.g.* in table 2.4 V_l = 4.08 V and V_h = 4.2 V corresponding to SoC_l = 90% and SoC_h = 100%, respectively.

When enough voltage and SoC intervals are chosen, this method will allow more flexibility (possibility of implementation for other types of battery) and precision in SoC estimation based on the EMF curve in comparison with a look-up table implementation. The problems of spread, temperature and aging remain to be solved.

(c) *Mathematical function.* In this method the EMF curve is approximated with a mathematical function. A possible example in which the EMF of an Li-ion battery with intercalated electrodes will be modelled as a difference in equilibrium potentials of positive and negative electrodes will be given in chapter 4 [1], [49].

Using an adaptive method for updating the equation parameters taking into consideration factors like spread, temperature and aging of the batteries, this method will probably offer the best solution for a practical EMF implementation.

Impedance measurements. The ratio of a complex voltage and a complex current is in general a complex quantity. The ratio *V/I* is generally denoted as the impedance *Z* (see for instance [50]). This definition is not always correctly applied in the battery-related literature. Impedance data on many practical battery designs are reported in [51]. A useful way of studying processes in electrochemical systems including biological processes, batteries and capacitors is to make impedance measurements over a wide range of frequencies, usually referred to as Electrochemical Impedance Spectroscopy (EIS).

The electrochemical impedance (or ac impedance) of a battery characterises its dynamic behaviour, that is, its response to an excitation of small amplitude. In principle, any type of excitation signal may be used (sine wave, noise, step, . . .). In practice, sine waves are however usually used. In galvanostatic (constant current) mode, the dc current *I* (polarization current) charging or discharging the battery is modified using a sinusoidal current:

$$\Delta I = I_{max} \sin(2\pi ft) \tag{2.3}$$

at frequency *f*, which is superimposed to *I*, yielding a sinusoidal voltage response:

$$\Delta V = V_{max} \sin(2\pi ft + \phi) \tag{2.4}$$

around the dc voltage *V* at the battery's terminals. The amplitude V_{max} and the phase angle ϕ depend on the frequency *f* and V_{max} also depends on the amplitude I_{max} of the applied ac current. In contrast, in potentiostatic mode (constant voltage), the dc voltage *V* at the battery's terminals is modified using a sinusoidal voltage

$$\Delta V = V_{max} \sin(2\pi ft) \tag{2.5}$$

at frequency *f*, which is superimposed onto *V*, yielding a sinusoidal current response:

$$\Delta I = I_{max} \sin(2\pi ft - \phi) \tag{2.6}$$

around the dc current *I* flowing through the battery. In this case, the amplitude I_{max} and the phase angle ϕ depend on the frequency *f* and I_{max} also depends on the amplitude V_{max} of the applied ac voltage. In both cases, the impedance is defined by

$$Z(f) = \frac{V_{\max}}{I_{\max}} e^{j\varphi} \tag{2.7}$$

Therefore, the electrochemical impedance of a battery is a frequency-dependent complex number characterised by either its real and imaginary parts or its modulus and phase angle ϕ.

It should be noted that the voltage amplitude V_{max} must not exceed about 10 mV to ensure that impedance measurements are performed under linear conditions. In this case the excitation and response signals are actually sine waves and the measured impedance does not depend on the amplitude of the excitation signal. Such a condition is easily fulfilled in potentiostatic mode with V_{max} being directly imposed by the experimenter. In galvanostatic mode, I_{max} must be determined so that V_{max} is close to 10 mV at all frequencies, especially at the lowest analysed frequency at which the modulus of the battery impedance is maximum. High power ac currents (of several A) may be required for high capacity batteries whose impedance values are in the mΩ range. Impedance diagrams may be presented as a Bode plot (modulus in log scale versus frequency and phase angle versus frequency) or, more frequently, a Nyquist plot (imaginary part versus real part). In the latter case, electrochemists generally plot the negative of the imaginary part on the ordinate axis, so that the capacitive loops appear in the upper quadrants. The general shape of the Nyquist diagram of the complex electrochemical impedance of a high-capacity LA battery cell is given in Fig. 2.10.

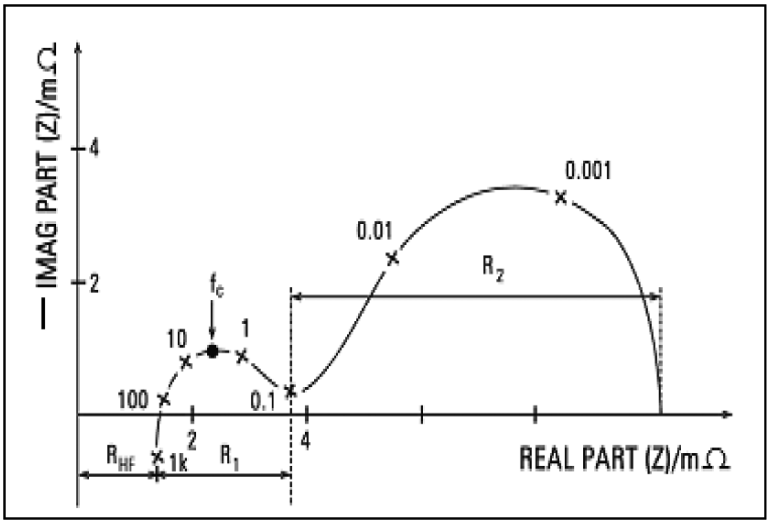

Fig. 2.10. Shape of the Nyquist diagram of the complex impedance of a high-capacity lead–acid battery cell (frequencies in Hz) [51].

The Nyquist diagram of Fig. 2.10 presents:

(a) an inductive part at frequencies higher than 100 Hz;
(b) a high-frequency resistance R_{HF} in the range of mΩ, which is the real part of the impedance at frequencies higher than 100 Hz;

(c) a first and small capacitive loop (size R_1) for frequencies between 0.1 and 100 Hz corresponding to the electrochemical reaction with the fastest kinetics;
(d) a second and large loop (size R_2) for frequencies lower than 0.1 Hz corresponding to the electrochemical reaction with the slowest kinetics.

Measurements of battery impedance as a function of frequency are not practical for SoC indication in a portable device because a signal with a frequency sweep has to be applied. Some dependence of the impedance on the SoC can be found in a laboratory set-up, but this dependence will usually be smaller than the dependence on a large temperature range as encountered in portable devices. The impedance measurements are used in portable products mainly as a means of indicating the battery's condition (SoH). Battery wear-out can be detected by an increase in the internal resistance, so the value of the internal resistance can be assessed by simply applying a current step to test whether the battery is of poor quality and should be replaced [1].

2.5.2 Book–keeping systems

Book-keeping is a method for SoC indication that is based on both current measurement and integration. This can be denoted as Coulomb counting, which literally means 'counting the charge flowing into or out of the battery'. These Coulomb counting data and other relevant data of the battery such as self-discharge rate, temperature, charge/discharge efficiency, history (*e.g.* cycle life), *etc*. will be used as input for the book-keeping system. The following Li-ion battery effects can be compensated for in a book-keeping system [1]:

Discharging 'efficiency'. Depending mainly on the SoC, T and I, only part of the available charge inside a battery can be retrieved. The main mechanisms behind this 'efficiency' are reaction kinetics and diffusion processes. These mechanisms involve reaction-rate and diffusion constants, which are temperature-dependent. Moreover, increased depletion of reacting species at the electrode surfaces occurs at larger currents and reaction-rate constants change over time as a battery ages. Consequently, a battery that may seem empty after it has been discharged with a relatively high current can still be discharged further after a rest period and/or with a lower current. In general, less charge can be obtained from a battery at low temperatures and/or large discharge currents. A battery's age also influences the discharging efficiency, for example due to increased internal resistance.

Self-discharge. Any battery will gradually loose charge, which will become apparent when a battery is left unused for some time. A Coulomb counter cannot measure this quantity of charge as no net current flows through the battery terminals. A battery's self-discharge rate will depend strongly on temperature and on the SoC.

Capacity loss. The maximum possible battery capacity in Ah decreases when a battery ages. The capacity loss depends on many factors. In general, the more the battery is misused, for example overcharged and overdischarged on a regular basis, the larger the loss will be. In most commercial book-keeping systems voltage measurement is often used to update the maximum battery capacity so as to deal with capacity loss [1].

The overall accuracy of 'Coulomb counting' depends on the accuracy of the current measurement across the full operating range of the battery system, in both the charging and discharging modes. Typically, the current measuring device measures the voltage across a shunt resistor connected in series to the battery system and converts the measured voltage into a current. This current is integrated and used to determine the SoC of the battery system. Higher current levels require substantially lower shunt resistor values and higher power dissipation ratings. The low resistance of such a shunt results in a very small voltage drop across the shunt, which must be measured in order to determine the smaller charge and discharge currents in the battery system. Since the function of the battery monitoring system is to provide time integration of the battery current in order to track the battery's SoC, even small errors in the measurement of the current can cause large errors in the SoC measurement to accumulate over time. One of the common errors when the signals to be measured are really small is the offset of the current measurement device.

A particular example of a book-keeping system for a mobile phone application is illustrated in Fig. 2.11 [52].

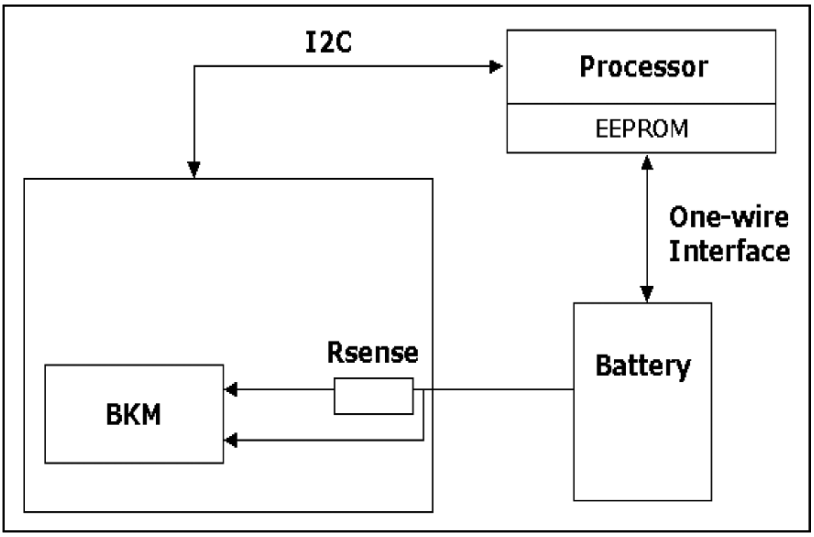

Fig. 2.11. Book-keeping system in a mobile phone application.

The book-keeping module (BKM) continuously monitors the battery and reports the obtained information (voltage, temperature, current measurements and integration) to the processor. The processor uses this information and the battery identification data to determine the SoC. The battery identification data consist of data allowing the determination of the battery's capacity. Those data are stored in the electrically erasable ROM (EEPROM) and are continuously updated by the processor. The processor uses one-wire interface to communicate with the battery. This means that the battery pack needs only three output connections: battery power, ground and one-wire interface.

The BKM can work in two different modes:

The sensitive mode. When a telephone is in idle mode, its consumption will be low, so greater accuracy will be needed to measure the current. The sensitive mode requires a measurement with high sensitivity.

The normal mode. During communication the consumption current is quite high in comparison with the idle mode. The normal mode is also used in the charge mode.

A high sensitivity, referred to as the lowest current value that needs to be measured, is very important for ensuring that all the charge flowing from and to a battery is monitored. The minor charge variations are not important for users, but they are essential for the system's reliability. The system must have some internal registers (see Fig. 2.12) that accumulate the minor variations. These registers are described below.

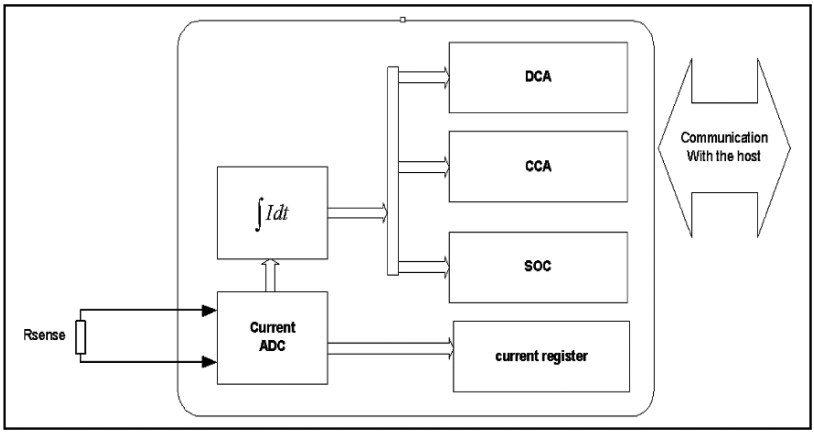

Fig. 2.12. Block diagram of the book-keeping support module (BKM).

Current register. Measurement of the current flowing into and out of a battery at the sampling moment.

SOC (SoC counter). Maintains a net accumulated charge flowing into and out of a battery. The reading in this register is an indication of the remaining capacity. This register is reset each time a low indication is given.

CCA (charging current accumulator). Accumulates the total charging current throughout a battery's life. It is only updated when the battery receives current.

DCA (discharging current accumulator). Accumulates the total discharging current throughout a battery's life. It is only updated when the battery provides current.

The DCA and CCA registers give information to the battery system needed to determine the end of life of the rechargeable battery based on total charge/discharge current throughout its lifetime.

2.5.3 Adaptive systems

The main problem in designing an accurate SoC indication system is the unpredictability of both battery behaviour and user behaviour. For this reason an adaptive system has to be used, which is based on direct measurement, book-

keeping or a combination of the two [1]. Some examples of existing adaptive SoC systems will be described in this section.

In [42], [53]–[55] optimum Kalman filters are presented for implementing an adaptive method in connection with parameter estimation to determine SoC. The basis of the filter is a numeric battery model description. In [42] the battery voltage is estimated on the basis of current and temperature measurements and then the results are compared with the measured battery voltage value (see Fig. 2.13). The inner (internal) parameter contains at least the SoC, but could also contain additional battery variables, such as an estimated value of the battery series resistance (which will give information on the battery's SoH). The model may contain the direct measurement function or the book-keeping function or a combination of the two. The system starts with a basic set of information describing standard behaviour of the type of battery concerned.

Adaptivity of the model is based on a comparison of the estimated values with observed battery behaviour. This comparison is made whenever possible. The purpose of a Kalman filter is to estimate a system's state on the basis of measurements, which contain errors. The filter has the advantage of being sequential – it needs only the system variables of the previous sample and the forcing terms and observations of the current sample.

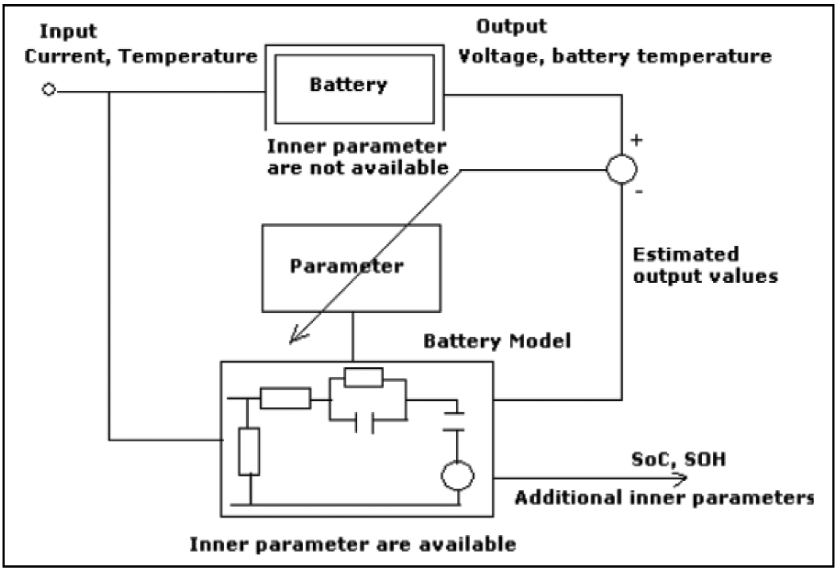

Fig. 2.13. Method for SoC and SoH determination using a Kalman filter [42].

In [53]–[55] Plett shows how the EKF (extended KF) may be used to adaptively identify unknown parameters in a cell model, in real-time, given cell voltage, current and temperature measurements. Five mathematical state-space models for modelling LiPB hybrid electrical vehicle (HEV) cell dynamics are discussed. The models with a single state are simple, but perform poorest. Adding hysteresis and filter states to the model improves performance, at some cost in complexity. The final model includes terms that describe the dynamic contributions due to open-circuit voltage, polarisation time constants, electrochemical hysteresis, ohmic loss and the effects of temperature. The results demonstrate that it is possible

to achieve a root-mean-squared modelling error that is smaller than the level of quantization error expected in an implementation. It is concluded that EKF provides the best solution for long-term SoC estimation [55].

[40] presents an application in which a battery's 'state variables' are replaced with neural weights with the aim of providing the portable equipment user with an accurate estimation of the remaining working time, *i.e*. how much time is left until the battery voltage reaches the cut-off value.

Two artificial neural networks (ANN), ANN_A and ANN_O, are used to model the system's implementation, more precisely to adapt the prediction of the current discharge curve to the general behaviour of the employed battery pack (see Fig. 2.14). An ANN requires at least two phases: a training phase to set the synaptic weights at those offering the 'best compromise' and an evaluation phase to test the accuracy of the ANN using previously unseen samples. 2860 discharge curves (260 cycles for 11 batteries) were used to train the system. It has been demonstrated that the ANN (even with online adaptation) can be useful even for small products. A mean error of about 3% has been found using this implementation method.

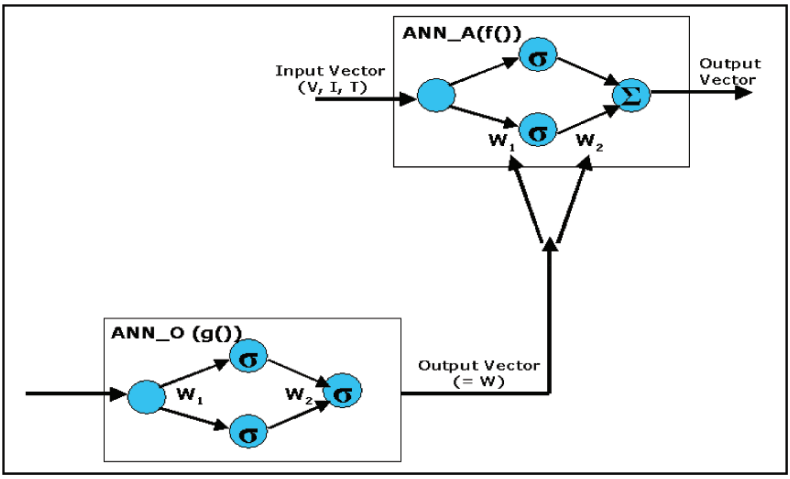

Fig. 2.14. Schematic representation of smart battery management using ANN [40].

[56] presents a method of SoC determination suitable for mobile communication applications. The effects of pulse current loads are investigated using a three-layer feed-forward artificial neural network, which is trained using the back propagation algorithm (for adjusting the weights and biases of each neuron on the basis of the error between SoC and the network's output). The paper demonstrates the use of artificial neural networks for characterising the discharge patterns for Li-ion batteries under pulsed loads typical of those required by the mobile telecommunications system.

In [41] SoC and SoH prediction based on fuzzy logic modelling is demonstrated for two battery systems, lithium–sulphur dioxide and NiMH. The method involves using fuzzy logic mathematics to analyse data obtained by impedance spectroscopy and/or Coulomb counting techniques. Data may be categorised by 'crisp' or 'fuzzy' sets. Crisp sets categorise data with certainty, *e.g.* a set of temperatures between 30°C and 40°C. With fuzzy sets, the set in which data can be categorised is uncertain, *e.g.* the temperature is 'warm'. This linguistic

descriptor ‘warm’ is a subset of a set of all temperatures and is defined by its membership function. The degree to which an element of the ‘temperature’ set belongs to the fuzzy subset ‘warm’ is indicated by a quantity referred to as its ‘degree of membership’ or fit fuzzy unit value.

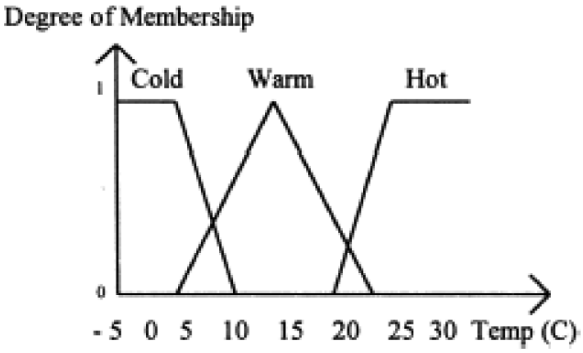

Fig. 2.15. Membership function for temperature.

Fig. 2.15 shows an example of three subsets, defined by their membership functions, ‘cold’, ‘warm’ and ‘hot’, of the ‘universe of discourse’ ‘temperature’ set. Using the above method for a limited data set the maximum error between the measured SoC and the model-predicted SoC obtained for lithium–sulphur dioxide cells was found to be +/– 5%.

2.5.4 Summary

A number of possible methods for SoC determination have been presented in this section. They were followed by descriptions of three of the best-known adaptive methods, which have as inputs measured battery variables such as voltage, impedance and current, and use these variables in order to accurately predict the SoC and the remaining time of use for an application. The SoC determination methods are summarised in Table 2.5 along with their fields of application, advantages and drawbacks [57].

Table 2.5. Overview of methods for SoC determination [57].

Technique	Field of application	Advantages	Drawbacks
Discharge test	Used for capacity determination at the beginning of life	Easy and accurate; independent of SoH	Offline, time-intensive, modifies the battery state, loss of energy
Coulomb counting	All battery systems, most applications	Accurate if enough re-calibration points are available and with good current measurements	Sensitive to parasite reactions; needs regular re-calibration points
OCV	Lead, Lithium, Zn/Br	Online, cheap, OCV prediction	Needs long rest time (current = 0)
EMF	Lead, Lithium	Online, cheap, EMF prediction	Needs long rest time (current = 0)
Linear model	Lead Photovoltaic	Online, easy	Needs reference data for fitting parameters
Impedance spectroscopy	All systems	Gives information on SoH and quality	Temperature sensitive, cost intensive
D. C. Internal resistance	Lead, NiCd	Gives information on SoH; possibility of online measurements	Good accuracy, but only for a short time interval
Artificial Neural Networks	All battery systems	Online	Needs training data of a similar battery, expensive to implement
Fuzzy logic	All battery systems	Online	Ask a lot of memory in real-word application
Kalman filters	All battery systems, PV, dynamic application	Online Dynamic	Difficult to implement the filtering algorithm that considers all features as *e.g.* nonnormalities and nonlinearities

2.6 Commercial State-of-Charge indication systems

The actual State-of-Charge technologies used by leading battery-management IC producers in practice will be presented in this section. Among those producers are Benchmarq/Unitrode/Texas Instruments, Dallas Semiconductor/Maxim, Linear Technology, PowerSmart/Microchip, Analog Devices, Xicor, Atmel and Mitsumi, to name but a few (see Table 2.6). Numerous manufacturers are offering SBS (smart battery system)-compatible [58] battery ICs, chargers and software drivers. These companies include AMI, Award Software, Hitachi, MCC, Microchip, O2 Micro, Phoenix Technologies, SystemSoft and VLSI Technologies.

Table 2.6. Main battery-management IC producers.

Texas Instruments Battery-management ICs	**Philips Semiconductors** Charge-control and monitor ICs	**Microchip Technology Inc** Battery-management ICs
Hitachi America Ltd Power-management μCs	**Zilog Inc** μC-based charge controller	**Integrated Circuit Systems Inc** Charge-control ICs
Linear Technology Corp Battery-management ICs	**Maxim Integrated Products** Charge-control ICs, SMBus-control ICs	**National Semiconductor Corp** Battery-management ICs
Analog Devices Battery-management ICs	**Xicor** Battery-management ICs	

Book-keeping Texas Instruments (TI) SoC ICs such as the bq2040, bq26220 [59], bq2060, bq2063 and many others are available on the market. In 2003, TI announced the release of its bq26500 battery fuel gauge – a SoC IC that incorporate an on-board processor to calculate the remaining battery capacity and system run-time (time-to-empty). The device measures the charge and discharge currents using an integrated low-offset voltage-to-frequency converter. A separate ADC on the IC is used to measure battery voltage and temperature. Two count registers accumulate charge and discharge counts, which are generated by sensing the voltage between the two sense resistor pins. Using the measurement inputs, the bq26500 runs a proven book-keeping algorithm (Coulomb counting that is also compensated for self-discharge and discharge rates) to accurately calculate remaining battery capacity and system run-time. The bq26500 compensates remaining battery capacity and run-times for temperature variations. The host system processor simply reads the data set in the bq26500 to retrieve remaining battery capacity, run-time and other critical information that is fundamental to comprehensive battery and power management, including available power, average current, temperature, voltage, time-to-empty and full charge [60]. In the TI ICs, a self-discharge count register counts at a rate of one count every hour at 25°C [61]. The self-discharge count rate doubles approximately every 10°C up to 60°C and is halved every 10°C below 25°C down to 0°C. This value is useful in estimating the battery self-discharge on the basis of capacity and storage temperature conditions.

The Microchip P3 SMBus Smart Battery ICs contain advanced battery control algorithms to determine remaining capacity, run-times and various other data relating to power-management systems [62]. These book-keeping algorithms also rely on a battery cell model that provides performance information of the particular chemical system in use. The cell models are often referred to as 'look-up tables' or LUTs. The look-up tables are stepwise approximations of the performance response curves that can be drawn when looking at discharge performance as a function of for example temperature and discharge rate. There are two look-up tables that define the predictive model for the lithium-ion cell chemistry. One look-up table predicts values of residual capacity (the capacity that cannot be removed from a battery due to discharging efficiency) that are used in remaining time calculations. The second is a predictive model of lithium self-discharge. The self-discharge parameter table predicts self-discharge rates as a function of temperature and total capacity loss. To create look-up tables from cell

data enough test points must be generated to create a series of curves that can be broken down into intervals to estimate the curvature with a stepwise approximation. Some LUT ‘tables’ are illustrated in Fig. 2.16.

The top left graphic in Fig. 2.16 represents the charge efficiency model for NiMH chemistry, the top right represents Li-ion discharge cell models. In the second row of the figure, the discharge performance and self-discharge of NiMH batteries are represented on the left and right, respectively.

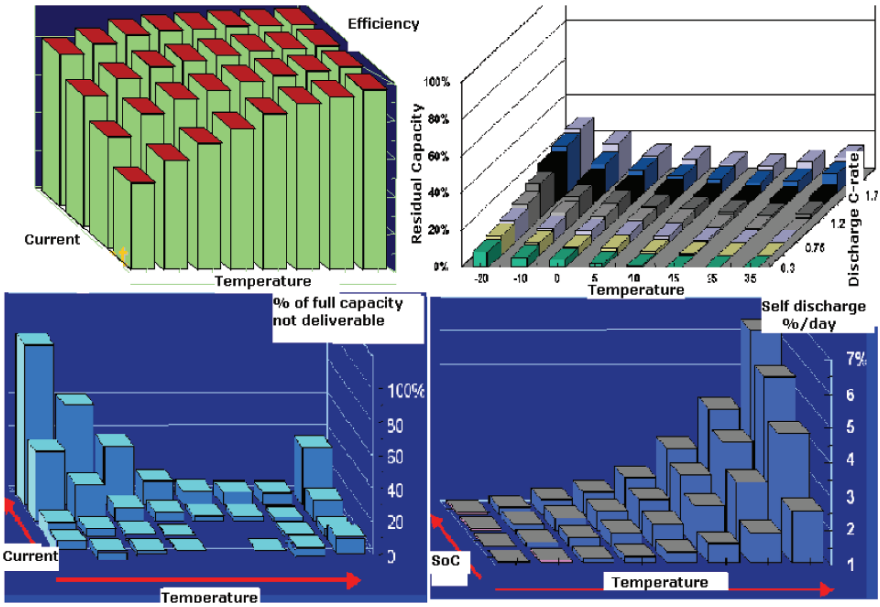

Fig. 2.16. Microchip 3D batteries models [63].

Maxim battery-management devices for Li-ion cells with a Coulomb counter, temperature converter and 15 bytes of user EEPROM, such as the DS2760 high-precision Li-ion battery monitor or 2438 integrated current accumulator (ICA), are available in practice. For the Maxim book-keeping algorithms to function accurately while minimising computational complexity and parametric data storage, certain assumptions are made.

Charge efficiency and pack self-discharge rate are assumed negligible in the case of Li-ion applications and are ignored [48]. The fuel gauging equations work by comparing the ICA value with expected ‘empty’ and ‘full’ values for that cell type, which are stored in the IC user EEPROM. These data are generated by characterising the cell type over the application’s expected temperature range and current consumption. This information is subsequently stored in a pack-resident memory for the algorithms to later extract and modify. Information should be gathered on several packs so that average or typical values can be stored in every production pack. For best accuracy, the data should be collected on assembled packs containing the production circuit as opposed to individual cells [48].

To collect the data, the cell pack is fully charged at each temperature and fully discharged at each rate and each temperature. All collected data points are arranged as shown in Table 2.7. Since only the difference between points is

important, the absolute values of the data do not matter, they have been normalised to the lowest value (standby current empty at 40°C). This reduces the number of data needed to be stored since standby empty 40°C is now always 0.

Table 2.7. Cell characterisation data.

	0°C	10°C	20°C	30°C	40°C
FULL (mAh)	554	561	578	582	588
STANDBY EMPTY (mAh)	65	42	19	11	0
ACTIVE EMPTY (mAh)	124	90	65	50	44

The active empty and standby empty points are defined as the capacity at which the battery reaches the empty voltage (as defined by the user) under the load of the active current and standby current, respectively [64]. The characterisation data are stored in two pages of the IC EEPROM memory. When characterisation of the cell pack is complete, calculating remaining capacity is very simple. The characterisation data are used to find the cell full and empty points on the basis of temperature and discharge rate.

The main drawback of all the discussed ICs is that none of them includes an adaptive method allowing for spread in battery and user behaviour, a large temperature and current range and aging of the cells under all realistic user conditions.

2.7 Conclusions

An overview of the state-of-the-art of State-of-Charge indication of rechargeable batteries, including a historical development of SoC technologies, has been given in this chapter. The general operational mechanism of batteries and the characteristics of the best-known three battery types were given in section 2.2.

The focus in section 2.3 was on the historical development of SoC indication. A general functional architecture of a SoC system was described in section 2.4.

Three basic methods for SoC indication were identified in section 2.5, including that of direct measurement. A particular direct measurement method is the EMF method. The advantage of this method is that the EMF curve does not depend on many parameters. The fact that it does not depend on aging or battery temperature, makes it potentially suitable for State-of-Charge indication. The main drawback of the EMF method is that it does not provide continuous indication of State-of-Charge.

A book-keeping system has been discussed with reference to a mobile phone application. The main problem in the case of book-keeping systems is defining reliable calibration opportunities that occur often enough during a battery's use [1].

Also described above are three of the best-known adaptive methods, which have as inputs measured battery variables such as voltage, impedance and current, and use these variables in order to accurately predict the SoC and the remaining time of use for an application. Using at least one of these adaptive systems should

improve a system's ability to cope with aging and temperature effects and spread in battery and user behaviour [1].

The focus in section 2.6 was on commercially available SoC systems. In this section a couple of the actual technologies used by most companies in practice were discussed. The drawback of all the discussed ICs is that none of them includes a real adaptive method allowing for spread in battery and user behaviour, a large temperature and current range and aging of the cells under all realistic user conditions.

2.8 References

[1] H.J. Bergveld, W.S. Kruijt, P.H.L. Notten, Battery Management Systems, Design by Modelling, Philips Research Book Series, **1**, Kluwer Academic Publishers, Boston (2002)
[2] I. Buchmann, Batteries in a Portable World, **2**, (2001)
[3] H. Zijlstra, F.F. Westendorp, Solid State Commun., **7**, 857 (1969)
[4] P.A. Boter, Rechargeable electrochemical cell, US Patent 4,004,943, filed 20 August (1975)
[5] H.J.H. van Deutekom, Rechargeable electrochemical cell, US Patent 4,214,043, filed 4 May (1978)
[6] P.H.L. Notten, J.R.G. van Beek, Nickel–metal hydride batteries: from concept to characteristics, Chem. Ind., **54**, 102–115 (2000)
[7] N. Furukawa, T. Ueda, Sanyo NiMH batteries outperform Li-ion, Nikkei Electronics Asia, 80–83 (1996)
[8] M. Broussely, S. Herreyre, P. Biensan, P. Kasztejna, K. Nechev, R.J. Staniewicz, Aging mechanism in Li-ion cells and calendar life predictions, J. Power Sources, **98**, 13–21 (2001)
[9] R. Spotnitz, Simulation of capacity fade in lithium-ion batteries, J. Power Sources, **113**, 72–80 (2003)
[10] P.M. Gomadam, J.W. Weidner, R.A. Dougal, R.E. White, Mathematical modeling of lithium-ion and nickel battery systems, J. Power Sources, **110**, 267–284 (2002)
[11] B.F.W.H. Heyer, One meter battery tester, US Patent 2,225,051, filed May 16 (1938)
[12] H. Dreer, Curtis wheelchair battery fuel gauge Product Test Report Marketing Services Dept., Curtis Instruments Inc., (1984)
[13] J.J. Kauzlarich, Electric wheelchair fuel gauge tests, Report No UVA-REC-102-86, UVA Rehabilitation Engineering Center (1986)
[14] Curtis Instruments, A Brief History of Innovation and Excellence, http://www.curtisinst.com/index.cfm?fuseaction=c Company.dspHistory, (2005)
[15] E.P. Finger, E.M. Marwell, Battery control system for battery operated vehicles, US Patent 4,012,681, filed 3 January (1975)
[16] S. Lerner, H. Lennon, H.N. Seiger, Development of an alkaline battery state of charge indicator, J. Power Sources, **3**, 135–137 (1970)
[17] R.A. York, Self-testing battery discharge indicator, US Patent 3,932,797, filed 24 December (1974)
[18] S. Kleineberg, M. Kauffmann, Method and circuit arrangement for determining the average current consumption of a battery-operated apparatus, US Patent 2005/0104559 A1, filed 17 February (2003)

[19] S. Hing, Device for estimating the state of charge of a battery, US Patent 6,529,840, filed 12 October (2000)
[20] T.J. Goedken, J.F. Goedken, Method and apparatus for detecting the state of charge of a battery, US Patent 5,185,566, filed 18 November (1991)
[21] R. Brandwein, M.L. Gupta, Nickel–cadmium battery monitor, US Patent 3,940,679, filed 18 June (1974)
[22] H. Laig-Horstebrock, E. Meissner, G. Richter, Method for determining the state of charge and loading capacity of an electrical storage battery, US Patent 6,362,598, filed 26 April (2001)
[23] C.C. Christianson, R.F. Bourke, Battery state of charge gauge, US Patent 3,946,299, filed 11 February (1975)
[24] R.L. Eby, Method and apparatus for determining the capacity of lead acid storage batteries, US Patent 4,180,770, filed 1 March (1978)
[25] S. Rodrigues, N. Munichandraiah, A.K. Shukla, A review of state-of-charge indication of batteries by means of a.c. impedance measurements, J. Power Sources, **87**, 12–20 (1999)
[26] E.J. Dowgiallo Jr., Method for determining battery state of charge by measuring A.C. electrical phase angle change, US Patent 3,984,762, filed 7 March (1975)
[27] E. Zaugg, Process and apparatus for determining the state of charge of a battery, US Patent 4,433,295, filed 8 January (1982)
[28] K. Muramatsu, Battery condition monitor and monitoring method, US Patent 4,678,998, filed 9 December (1985)
[29] E. Peled, H. Yamin, I. Reshef, D. Kelrich, S. Rozen, Method and apparatus for determining the state-of-charge of batteries particularly lithium batteries, US Patent 4,725,784, filed 10 September (1984)
[30] U. Kopmann, Method of and apparatus for monitoring the state of charge of a rechargeable battery, US Patent 4,677,363, filed 30 June (1987)
[31] L. Bowen, R. Zarr, S. Denton, A microcontroller-based intelligent battery system, IEEE AES System Magazine, 16–19 (1994)
[32] E.P. Finger, Quiescent voltage sampling battery state of charge meter, US Patent 4,460,870, filed 23 July (1981)
[33] Y. Tanjo, T. Nakagawa, H. Horie, T. Abe, K. Iwai, M. Kawai, State of charge indicator, US Patent 6,127,806, filed 14 May (1999)
[34] J.H. Aylor, A. Thieme, B.W. Johnson, A battery state-of-charge indicator for electric wheelchairs, IEEE Trans. Indust. Electron., **39**, 398–409 (1992)
[35] T. Kikuoka, H. Yamamoto, N. Sasaki, K. Wakui, K. Murakami, K. Ohnishi, G. Kawamura, H. Noguchi, F. Ukigaya, System for measuring state of charge of storage battery, US Patent 4,377,787, filed 8 August (1980)
[36] G.R. Seyfang, Battery state of charge indicator, US Patent 4,949,046, filed 21 June (1988)
[37] M.W. Verbrugge, E.D. Tate Jr, S.D. Sarbacker, B.J. Koch, Quasi-adaptive method for determining a battery's state of charge, US Patent 6,359,419, filed 27 December (2000)
[38] G. Richter, E. Meissner, Method for determining the state of charge of storage batteries, US Patent 6,388,450, filed 15 December (2000)
[39] D. Stolitzka, W.S. Dawson, When is it intelligent to use a smart battery?, No 94 TH0617-1 IEEE, (1994)

[40] O. Gerard, J.N. Patillon, F. d'Alche-Buc, Neural network adaptive modelling of battery discharge behaviour, Lect. Notes Comput. Sci., **1327**, 1095–1100 (1997)
[41] A.J. Salkind, C. Fennie, P. Singh, T. Atwater, D.E. Reisner, Determination of state-of-charge and state-of-health of batteries by fuzzy logic methodology, J. Power Sources, **80**, 293–300 (1999)
[42] J. Garche, A. Jossen, Battery management systems (BMS) for increasing battery life time, Telecommunications Energy Special, **3**, 81–84 (2000)
[43] H.J. Bergveld, H. Feil, J.R.G.C.M. Van Beek, Method of predicting the state of charge as well as the use time left of a rechargeable battery, US Patent 6,515,453, filed 30 November (2000)
[44] F.A.C.M. Schoofs, W.S. Kruijt, R.E.F. Einerhand, S.A.C. Hanneman, H.J. Bergveld, Method of and device for determining the charge condition of a battery, US Patent 6,420,851, filed 29 March (2000)
[45] P.P.L. Regtien, F. van der Heijden, M.J. Korsten, W. Olthuis, Measurement Science for Engineers, Kogan Page Science Publisher, London (2004)
[46] D. Linden, Handbook of batteries, 2nd edition, McGraw-Hill, New York, (1995)
[47] Dallas Semiconductors, Inaccuracies of estimating remaining cell capacity with voltage measurements alone, Application Note 121, (2000)
[48] Dallas Semiconductors, Lithium-ion cell fuel gauging with Dallas semiconductor devices, Application Note 131, (2000)
[49] G.A. Nazri, G. Pistola, Science and Technology of Lithium Batteries (2002)
[50] P.P.L. Regtien, Instrumentation Electronics, Prentice-Hall, New York, (1992)
[51] F. Huet, A review of impedance measurements for determination of the state-of-charge or state-of-health of secondary batteries, J. Power Sources, **70**, 59–69 (1998)
[52] Philips Internal Communications, (2005)
[53] G. Plett, Extended Kalman filtering for battery management systems of LiPB-based HEV battery packs: Part 1. Background, J. Power Sources, **134**, 252–261 (2004)
[54] G. Plett, Extended Kalman filtering for battery management systems of LiPB-based HEV battery packs: Part 2. Modeling and identification, J. Power Sources, **134**, 262–276 (2004)
[55] G. Plett, Extended Kalman filtering for battery management systems of LiPB-based HEV battery packs: Part 3. State and parameter estimation, J. Power Sources, **134**, 277–292 (2004)
[56] S. Grewal, D.A. Grant, A novel technique for modelling the state of charge of lithium ion batteries using artificial neural networks, Proc. Int. Telecommunications Energy Conf. (IEEE), **484**, 14–18 (2001)
[57] S. Piller, M. Perrin, A. Jossen, Methods for state-of-charge determination and their applications, J. Power Sources, **96**, 113–120 (2001)
[58] D. Friel, M. Mattera, SBS smart battery interface guidelines, Portable and Wireless (1998)
[59] Texas Instruments, High-performance battery monitor IC with Coulomb counter, voltage and temperature measurements, Doc. I.D. SLUS521A (2002)
[60] Texas Instruments, Single-cell Li-ion and Li-Pol battery gas gauge IC for handheld applications (bq junior family), Doc. I.D. SLUS567A (2003)
[61] Texas Instruments, High-performance battery monitor with coulomb counting and flash memory, Doc. I.D. SLUS509 (2001)

[62] Power Smart, P3 cell model explanations, Application Note 450799 (1999)
[63] L. Conklin, Smart battery data accuracy, Intel Developer Forum (1999)
[64] Dallas Semiconductors, Characterizing a Li+ cell for use with a fuel cell, Application Note 2412 (2003)